

Supplementary Material: Narrowband Mid-infrared reflectance filters using guided mode resonance

*Anil K. Kodali,^{1,2,3} Matthew Schulmerich,^{2,3,5} Jason Ip,^{3,5} Gary Yen,^{3,4} Brian T. Cunningham,^{3,4} and
Rohit Bhargava^{2,3,5,*}*

¹Department of Mechanical Science and Engineering, ²Beckman Institute for Advanced Science and
Technology, ³Micro and Nanotechnology Laboratory, ⁴Electrical and Computer Engineering, and
⁵Department of Bioengineering, University of Illinois at Urbana-Champaign, Urbana, Illinois, 61801,
USA.

*To whom correspondence should be addressed, rxb@illinois.edu.

The details of the formulation of continuity conditions and systems of equations that govern the coefficients in coupled wave expansions for fields in each layer are provided here. A discussion of the applicability of the filters for various incidence angles apart from the normal incidence is also provided. The results show that the proposed filters can be used for polarization selection at several distinct regions and with different band-widths in mid-IR.

SUPPORTING INFORMATION

Systems of equations: integrating model parameters with optical theory

In the substrate region, similarly, there is only a forward-wave component. Accordingly the quantities A^c and B^s vanish. The field in the cover region is due to both \mathbf{E}^c and the incident field \mathbf{E}^{inc} and the field in the substrate region is only due to \mathbf{E}^s . Other specific relationships are:

At the cover(c)-grating(gr) layer interface ($z=0$):

$$-\sin \phi_p M_{x,p}(0) + \cos \phi_p M_{y,p}(0) = \sin \psi \delta_{p0} + \left\{ -\sin \phi_p B_{x,p}^c + \cos \phi_p B_{y,p}^c \right\}$$

$$\begin{aligned} & \cos \phi_p M_{x,p}(0) + \sin \phi_p M_{y,p}(0) \\ &= \cos \psi \cos \theta - \left(\frac{s_z^c}{\varepsilon^c(\nu)} \right) \left\{ \begin{array}{l} (p \cos \phi_p s_z^c) B_{x,p}^c \\ -(\sin \phi_p s_z^c) B_{y,p}^c - (\cos \phi_p s'_{x,p} + \sin \phi_p s_y) B_{z,p}^c \end{array} \right\} \end{aligned}$$

$$\cos \phi_p N_{x,p}(0) + \sin \phi_p N_{y,p}(0) = i \left\{ \begin{array}{l} \sqrt{\varepsilon^c(\nu)} \sin \psi \cos \theta - \\ s_z^c (-\sin \phi_p B_{x,p}^c + \cos \phi_p B_{y,p}^c) \end{array} \right\} \quad (i)$$

$$\begin{aligned} & \sin \phi_p N_{x,p}(0) - \cos \phi_p N_{y,p}(0) \\ &= i \left[\sqrt{\varepsilon^c(\nu)} + \left\{ \begin{array}{l} (p \cos \phi_p s_z^c) B_{x,p}^c \\ -(\sin \phi_p s_z^c) B_{y,p}^c - (\cos \phi_p s'_{x,p} + \sin \phi_p s_y) B_{z,p}^c \end{array} \right\} \right] \end{aligned}$$

where the inclination angle of the diffracted mode is given by: $\phi_p = \tan^{-1}(s_y/s'_{x,p})$.

At the grating(gr)-waveguide(wg) layer interface ($z=d^{\text{gr}}$):

$$-\sin \phi_p M_{x,p}(d^{\text{gr}}) + \cos \phi_p M_{y,p}(d^{\text{gr}}) = \left\{ -\sin \phi_p A_{x,p}^{\text{wg}} + \cos \phi_p A_{y,p}^{\text{wg}} \right\} + \left\{ -\sin \phi_p B_{x,p}^{\text{wg}} + \cos \phi_p B_{y,p}^{\text{wg}} \right\}$$

$$\begin{aligned}
& \cos \phi_p M_{x,p}(d^{sr}) + \sin \phi_p M_{y,p}(d^{sr}) \\
&= \left(\frac{s_z^{wg}}{\varepsilon^{wg}(v)} \right) \left\{ (p \cos \phi_p s_z^{wg}) A_{x,p}^{wg} - (\sin \phi_p s_z^{wg}) A_{y,p}^{wg} \right. \\
&\quad \left. - (\cos \phi_p s'_x + \sin \phi_p s_y) A_{z,p}^{wg} \right\} \\
&\quad + \left(\frac{s_z^{wg}}{\varepsilon^{wg}(v)} \right) \left\{ (p \cos \phi_p s_z^{wg}) B_{x,p}^{wg} - (\sin \phi_p s_z^{wg}) B_{y,p}^{wg} \right. \\
&\quad \left. - (\cos \phi_p s'_x + \sin \phi_p s_y) B_{z,p}^{wg} \right\}
\end{aligned}$$

$$\begin{aligned}
& \cos \phi_p N_{x,p}(d^{sr}) + \sin \phi_p N_{y,p}(d^{sr}) \\
&= i \left\{ -s_z^{wg} \left(-\sin \phi_p A_{x,p}^{wg} + \cos \phi_p A_{y,p}^{wg} \right) - s_z^{wg} \left(-\sin \phi_p B_{x,p}^{wg} + \cos \phi_p B_{y,p}^{wg} \right) \right\} \quad (ii)
\end{aligned}$$

$$\begin{aligned}
& \sin \phi_p N_{x,p}(d^{sr}) - \cos \phi_p N_{y,p}(d^{sr}) \\
&= i \left\{ \left[(p \cos \phi_p s_z^{wg}) A_{x,p}^{wg} - (\sin \phi_p s_z^{wg}) A_{y,p}^{wg} - (\cos \phi_p s'_x + \sin \phi_p s_y) A_{z,p}^{wg} \right] \right. \\
&\quad \left. + \left[(p \cos \phi_p s_z^{wg}) B_{x,p}^{wg} - (\sin \phi_p s_z^{wg}) B_{y,p}^{wg} - (\cos \phi_p s'_x + \sin \phi_p s_y) B_{z,p}^{wg} \right] \right\}
\end{aligned}$$

At the waveguide(wg)-substrate(s) interface ($z=d^{sr}+d^{wg}$):

$$A_{x,p}^s = A_{x,p}^{wg} \exp\{i2\pi v s_z^{wg} d^{wg}\} + B_{x,p}^{wg}$$

$$A_{y,p}^s = A_{y,p}^{wg} \exp\{i2\pi v s_z^{wg} d^{wg}\} + B_{y,p}^{wg}$$

(iii)

$$(s_y A_{z,p}^{wg} - s_z^{wg} A_{y,p}^{wg}) \exp\{i2\pi v s_z^{wg} d^{wg}\} + s_y B_{z,p}^{wg} + s_z^{wg} B_{y,p}^{wg} = s_y B_{z,p}^s - s_z^s B_{y,p}^s$$

$$(s_z^{wg} A_{x,p}^{wg} - s'_x A_{z,p}^{wg}) \exp\{i2\pi v s_z^{wg} d^{wg}\} - s_z^{wg} B_{x,p}^{wg} + s'_x B_{z,p}^{wg} = s_z^s B_{x,p}^s - s'_x B_{z,p}^s$$

For a system which considers N_F coefficients for series expansions, hence, there are $24N_F$ coefficients. $6N_F$ of these coefficients are assigned a value of zero (all A^c and B^s). Consequently, $12N_F$ independent equations are obtained from (i-iii) and $6N_F$ equations are obtained from transversality conditions.

Transversality Conditions:

In the grating region, the electric and magnetic fields can be relating using Maxwell's equations:

$$\mathbf{E}^{\text{gr}} = \frac{i}{2\pi v \epsilon(x)} \sqrt{\frac{\mu_0}{\epsilon_0}} \nabla \times \mathbf{H}^{\text{gr}}, \quad \mathbf{H}^{\text{gr}} = \frac{-i}{2\pi v} \sqrt{\frac{\epsilon_0}{\mu_0}} \nabla \times \mathbf{E}^{\text{gr}}, \quad (\text{iv})$$

Using (iv) in the expression for field description in grating layer provided in the manuscript and eliminating $\mathbf{M}_z(z)$ and $\mathbf{N}_z(z)$, a finite system of differential equations can be obtained as follows for all modes:

$$\begin{bmatrix} \frac{\partial \mathbf{M}_x}{\partial z} \\ \frac{\partial \mathbf{M}_y}{\partial z} \\ \frac{\partial \mathbf{N}_x}{\partial z} \\ \frac{\partial \mathbf{N}_y}{\partial z} \end{bmatrix} = i2\pi v \begin{bmatrix} 0 & 0 & \mathbf{S}_y \boldsymbol{\epsilon}^{-1} \mathbf{S}_x & \mathbf{I} - \mathbf{S}_y \boldsymbol{\epsilon}^{-1} \mathbf{S}_y \\ 0 & 0 & \mathbf{S}_x \boldsymbol{\epsilon}^{-1} \mathbf{S}_x - \mathbf{I} & -\mathbf{S}_x \boldsymbol{\epsilon}^{-1} \mathbf{S}_y \\ \mathbf{S}_x \mathbf{S}_y & \boldsymbol{\epsilon} - \mathbf{S}_y^2 & \mathbf{0} & \mathbf{0} \\ \mathbf{S}_x^2 - \boldsymbol{\epsilon} & -\mathbf{S}_x \mathbf{S}_y & \mathbf{0} & \mathbf{0} \end{bmatrix} \begin{bmatrix} \mathbf{M}_x \\ \mathbf{M}_y \\ \mathbf{N}_x \\ \mathbf{N}_y \end{bmatrix} \quad (\text{v})$$

where \mathbf{S}_x and \mathbf{S}_y are diagonal matrices with diagonal elements $s_{x,p}^{\text{gr}}$ and $s_{y,p}^{\text{gr}}$ respectively and $\boldsymbol{\epsilon}$ is a matrix in which $\boldsymbol{\epsilon}_{jh} = \epsilon_{j-h}^{\text{gr}}$. This set of equations is solved using an Eigen decomposition of the matrix involved in equation (v) in the form of $\mathbf{G}\boldsymbol{\Gamma}\mathbf{G}^{-1}$, where $\boldsymbol{\Gamma}$ is a diagonal matrix with Eigen values in the diagonal and columns of matrix \mathbf{G} are the corresponding Eigen vectors. With this decomposition, a solution set can be constructed as:

$$\begin{aligned} \mathbf{M}_{xp} &= \sum_{j=1}^{N_F} \{ \alpha_j \mathbf{g}_{j,p} \exp[i2\pi v \gamma_j z] + \beta_j \tilde{\mathbf{g}}_{j,p} \exp[i2\pi v \gamma_j (d_{\text{gr}} - z)] \}, \\ \mathbf{M}_{yp} &= \sum_{j=1}^{N_F} \{ \alpha_j \mathbf{g}_{j,p+N_F} \exp[i2\pi v \gamma_j z] + \beta_j \tilde{\mathbf{g}}_{j,p+N_F} \exp[i2\pi v \gamma_j (d_{\text{gr}} - z)] \}, \\ \mathbf{N}_{xp} &= \sum_{j=1}^{N_F} \{ \alpha_j \mathbf{g}_{j,p+2N_F} \exp[i2\pi v \gamma_j z] + \beta_j \tilde{\mathbf{g}}_{j,p+2N_F} \exp[i2\pi v \gamma_j (d_{\text{gr}} - z)] \}, \end{aligned} \quad (\text{vi})$$

$$N_{yP} = \sum_{j=1}^{N_F} \{ \alpha_j \mathbf{g}_{j,P+3N_F} \exp[i2\pi v \gamma_j z] + \beta_j \tilde{\mathbf{g}}_{j,P+3N_F} \exp[i2\pi v \gamma_j (d_{gr} - z)] \},$$

where $\mathbf{g}_{j,p}$ is element of j^{th} Eigen vector column that corresponds to the positive Eigen value γ_j and similarly $\tilde{\mathbf{g}}_{j,p}$ is Eigen vector value corresponding to Eigen value $-\gamma_j$. $\mathbf{M}_z(z)$ and $\mathbf{N}_z(z)$ can be obtained using equation (vi), in the following expression eliminated to obtain (v):

$$\mathbf{M}_{z,p} = -\frac{1}{2\pi v} \left[\sum_{p''} \eta_{p-p''} \left\{ \mathbf{s}_{xp}^{\text{gr}} N_{yp''} \right\} \right], \quad (\text{vii})$$

$$\mathbf{N}_{z,p} = \frac{1}{2\pi v} \left[\mathbf{s}_{xp}^{\text{gr}} M_{yp''} \right],$$

where η_h are the Fourier coefficients of inverse of the dielectric function ϵ^{gr} . Substituting M and N into equations (i) and (ii), they can be expressed in terms of unknown coefficients α_j and β_j .

In addition, in the homogeneous layers, Gauss's equation results in conditions:

$$\mathbf{s}'_x \mathbf{A}_x^{\mathcal{L}} + \mathbf{s}'_y \mathbf{A}_y^{\mathcal{L}} + \mathbf{s}^{\mathcal{L}}_z \mathbf{A}_z^{\mathcal{L}} = \mathbf{0}, \quad (\text{viii})$$

$$\mathbf{s}'_x \mathbf{B}_x^{\mathcal{L}} + \mathbf{s}'_y \mathbf{B}_y^{\mathcal{L}} - \mathbf{s}^{\mathcal{L}}_z \mathbf{B}_z^{\mathcal{L}} = \mathbf{0},$$

Equations (vi-viii) thus provide for the required $6N_F$ equations.

This set of equations is then solved using a standard matrix decomposition (LU or QR) method. The fields can then be explicitly calculated using the obtained coefficients.

Filter Responses at different angles of incidence:

At oblique incidences, the higher order guided modes lead to resonances in the reflection responses of the proposed filters.

Figure S 1 depicts the reflectance spectra of filters for TM and TE polarized beams at three different angles of incidence ($\theta = 30^\circ, 45^\circ, 60^\circ$). Both experimental results and theoretical predictions are presented. The angles of incidence are slightly modified for obtaining a closer match between the simulations and experimental results. However, for a particular structure over TE and TM polarized

incidences, only the polarizer has been adjusted to a different setting while recording the measurements. Keeping this in mind, a single modified θ value has been used for a particular structure for the simulation results of different polarizations. In all cases the azimuthal angle of incident beam has been assumed to be 0. The peak locations obtained are proximal to those predicted by theory. In some cases, the expected higher side-bands do not exist. The differences in peak locations could be due to substrate effects, non-rectangular profile of ridges and grooves in grating layer and surface imperfections. The differences in peak heights could be due to variability of rays in the beam, non-zero azimuthal angle, and a probably higher absorption index of the material. The filter responses can thus be verified over different angles of incidence, but a thorough study is required to accurately model the variability. Nevertheless, the results show that these filters can be used as polarization-selective reflectance filters at several distinct regions and with different bandwidths in mid-IR.

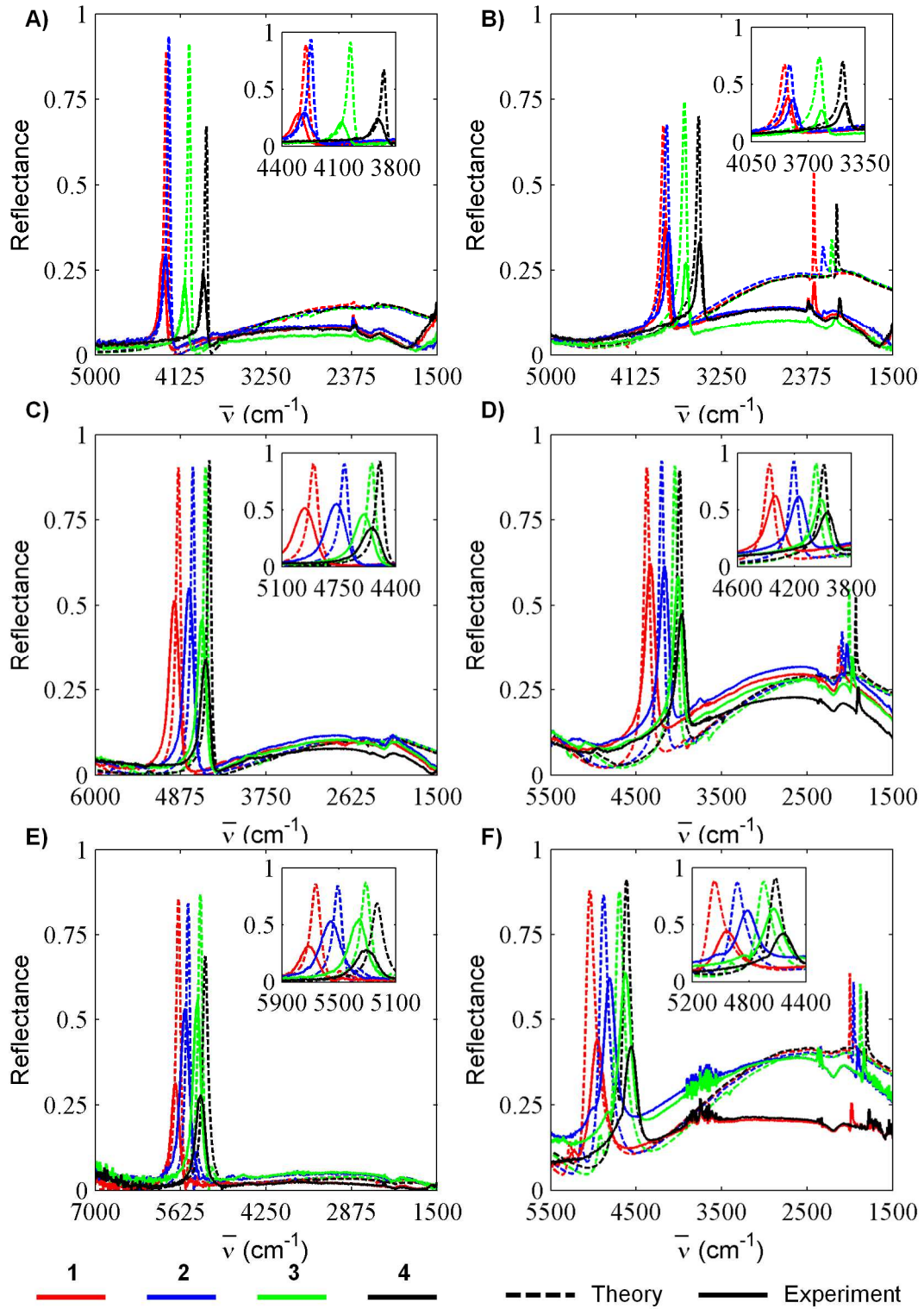


Figure S 1: Reflectance Spectra of filters for TM-polarized incidences at $\theta = 30, 45, 60^\circ$ (A, C, E) and for TE-polarized incidences at $\theta = 30, 45, 60^\circ$ (B, D, F). The angles have been slightly modified for a close match between experimental results and theoretical predictions. The corresponding θ values

chosen for structures 1, 2, 3 and 4 respectively are for 30^0 - (28.5, 30.2, 29.5, 28.5), for 45^0 -(41, 39.5, 39.8, 41.5) and for 60^0 - (56.5, 55.5, 55.5, 57).